IEEE Access
Multidisciplinary | Rapid Review | Open Access Journal

Received September 16, 2018, accepted October 16, 2018, date of publication October 22, 2018,
date of current version November 19, 2018.

Digital Object Identifier 10.1109/ACCESS.2018.2877252

QAM Signal Transmission Based on Matrix Model in Filter-Bank Multicarrier Systems

FEI LI[1], (Student Member, IEEE), KAN ZHENG[1], (Senior Member, IEEE), HUI ZHAO[1], AND WEI XIANG[2], (Senior Member, IEEE)

[1]School of Information and Communication Engineering, Beijing University of Posts and Telecommunications, Beijing 100876, China
[2]College of Science and Engineering, James Cook University, Townsville, QLD 4814, Australia

Corresponding author: Kan Zheng (zkan@bupt.edu.cn)

This work was supported by the National Nature Science Foundation of China (NSFC) under Grant 61628102 and Grant 61271183.

ABSTRACT In the upcoming fifth-generation (5G) mobile network, the filter bank multi-carrier (FBMC) technique provides an alternative to cyclic prefix-orthogonal frequency-division multiplexing (CP-OFDM). The most fascinating features of FBMC are high spectral efficiency and extremely low out-of-band emissions by removing the CP and using well-localized pulse shapes. FBMC exhibits intrinsic inter-carrier/inter-symbol interference which can be mitigated by techniques such as offset quadrature amplitude modulation (OQAM). However, OQAM does not work well in multi-path fading channels. Consequently, conventional channel estimation methods and MIMO based upon space–time/frequency block coding are not straightforward applicable to the FBMC system. This paper presents two new transceiver architectures for the FBMC/QAM matrix. First of all, the matrix models of the FBMC/QAM scheme are derived. Second, based on the matrix models, three receiver methods are then described. Then, the scheme of combining FBMC/QAM with channel estimation and MIMO is proposed. Finally, two simplified receiver algorithms based on the matrix models are proposed. Simulation results indicate that the proposed transceivers of the FBMC/QAM matrix scheme can directly combine with the channel estimation and MIMO techniques used in conventional OFDM systems. Furthermore, the proposed transceivers of the FBMC/QAM matrix scheme have almost the same BER performance compared with the conventional OFDM systems.

INDEX TERMS Multicarrier, FBMC, QAM, channel estimation, MIMO, complexity.

I. INTRODUCTION

Cyclic prefix-orthogonal frequency division multiplexing (CP-OFDM) [1] as a physical layer interface has been widely used in today's digital communication systems. The CP of OFDM improves robustness against impairments caused by multi-path fading [2]. Unfortunately, this is achieved at the expense of spectral efficiency. Moreover, due to the high out-of-band (OOB) emissions caused by the rectangular pulse shape, OFDM cannot support effective asynchronous access.

Among many new multi-carrier technologies, filter bank multi-carrier (FBMC) [3]–[5] utilizes well-localized pulse shapes to reduce the OOB emissions. It also has the advantage of high spectral efficiency by removing the CP. Moreover, FBMC does not need strict synchronization [6], [7]. The attractive features of FBMC come at the expense of the intrinsic inter-carrier interference (ICI) and inter-symbol interference (ISI). In order to mitigate intrinsic interference, FBMC employs offset quadrature amplitude modulation (OQAM) to transmit the real and imaginary parts of complex-valued symbols. Although OFDM transmits QAM symbols directly, the real or imaginary part of a FBMC/OQAM symbol is delayed only by half of the symbol duration, so that the symbol rate is twice as fast as OFDM. Therefore, they can achieve similar spectral efficiency [8].

However, the complex-valued response of the channel destroys the real orthogonality of OQAM, resulting in that FBMC/OQAM cannot accurately estimate the channel. Therefore, some preamble-based channel estimation methods are proposed in [9]–[12]. Although these methods can indeed solve the channel estimation problem of FBMC/OQAM, the combination of OQAM and MIMO proves a challenging research problem.

Lin *et al*. [13] propose a CP-OQAM pseudo-Alamouti transceiver, but this scheme requires additional CP, which degrades the spectral efficiency. Moreover, the combination of OQAM and MIMO [14]–[16] inherently has

many disadvantages. Thus, some combined QAM and MIMO solutions have been proposed. Zakaria and Ruyet [17] propose to transmit complex-valued symbols alternated with null data, which can transform two-dimensional inter-symbol interference into one-dimensional inter-symbol interference. However, the bit error rate (BER) performance of FBMC in [17] is still worse than that of OFDM. In [18], an iterative interference cancellation MLD receiver was proposed to perform per-tone MLD without performance degradation. In [19], a FBMC system that can transmit QAM symbols is proposed. It utilizes two filters on odd and even numbered sub-carriers to eliminate interference. However, the orthogonality conditions of FBMC/QAM do not hold perfectly under multipath fading channels [20], [21]. Moreover, the FBMC/QAM system mentioned in [19] has larger OOB emissions compared with the OFDM systems. In [22], FFT-FBMC is proposed without intrinsic interference in MIMO system. However, the FFT-FBMC system needs additional CP and also has the worse BER performance compared to OFDM. Lélé *et al.* [23] propose use Alamouti coding in conjunction with OFDM/OQAM, but only when it is combined with code division multiple access (CDMA).

Internet of Things (IoT) and machine-type-communication (MTC) will play an important role in future wireless communication systems. These application scenarios are mainly short packet transmission. Therefore, the waveform demands efficient support of short transmission bursts. Moreover, in order to achieve efficient bandwidth traffic, the next generation systems also need to support multi-antenna technology, i.e., MIMO.

In this paper, a new transceiver model for FBMC/QAM is proposed. The characteristics of the proposed model can be summarized as follows. The transmitter directly transmits the QAM symbol, and the functional blocks, such as upsample, multi-carrier modulation and pulse shaping, can be described by matrix operations. Based on the FBMC/QAM scheme, a transmitter architecture that is more suitable for IoT and MTC communications is also proposed, i.e., cycle superimposition-FBMC/QAM (CS-FBMC/QAM). The proposed architecture can directly apply existing channel estimation and MIMO technology, which makes it easier to combine FBMC and MIMO. In addition, CS-FBMC/QAM has shorter transmission bursts than OFDM, which can benefit scenarios such as IoT and low latency. The corresponding receiver based on the transmitter have three standard means of detecting the signal, i.e., the matched filter (MF), zero forcing (ZF) and minimum mean square error (MMSE), which are different operations of the transmitter matrix. What's more, the impact on the performance of the receiver is compared in terms of different pulse shaping filters. Meanwhile, the combination of existing techniques (i.e., channel estimation and MIMO) and the proposed FBMC/QAM and CS-FBMC/QAM is also analyzed and simulated. Besides, based on the ZF receiver, a low-complexity implementation of the FBMC/QAM and CS-FBMC/QAM scheme is designed finally.

The remainder of this paper is organized as follows. The FBMC/OQAM system model is reviewed in Section II. Section III describes the transceiver of the proposed FBMC/QAM and CS-FBMC/QAM scheme. Channel estimation and MIMO are presented in Sections IV and V, respectively. The low complexity implementation is detailed in Section VI. Section VII presents the simulation results, followed by concluding remarks drawn in Section VIII.

II. FBMC/OQAM SYSTEM MODEL

The system model of FBMC/OQAM is reviewed in this section. The baseband equivalent of a discrete-time signal at the output of the FBMC/OQAM transmitter can be written as follows [24]

$$s(l) = \sum_{m=0}^{M-1} \sum_{n=0}^{N-1} a_{m,n} g_{m,n}(l), \tag{1}$$

where $l \in \mathbb{Z}$ is the sample index, $a_{m,n}(n = 0, 1, \ldots, N-1, n \in \mathbb{Z})$ denotes the symbol transmitted by the sub-carrier of index n during the m'th symbol time. $g_{m,n}(l)$ represents the time and frequency shifted version of the prototype function $g(l)$, which can be expressed as

$$g_{m,n}(l) = e^{j\frac{2\pi nl}{N}} g\left(l - \frac{mN}{2}\right), \tag{2}$$

where $\frac{mN}{2} \le l \le \frac{mN}{2} + KN - 1$, K is the upsample factor, and generally $K = 4$.

Let $\mathbf{r}$ be the vector of time samples $r[n]$ at the receiver. Further, denote by $\mathbf{w} \sim \mathbb{N}\left(0, \sigma_{\mathbf{n}}^2\right)$ the additive white Gaussian noise (AWGN). At the receiver side, the received signal can be expressed as

$$\mathbf{r} = \mathbf{H}\mathbf{s} + \mathbf{w}, \tag{3}$$

where $\mathbf{s}$ is the vector of $s(l)$, $\mathbf{H}$ denotes the channel. In AWGN channels, we have H = I, hence $\mathbf{r} = \mathbf{s} + \mathbf{w}$. For Rayleigh multipath channels, $\mathbf{H}$ is a convolution matrix constructed from a channel response $h(n)$ with an exponential power delay profile.

Before frequency domain equalization (FDE) and OQAM demodulation, the desired signal for the n's sub-carrier at time m can be described as

$$\hat{a}_{m,n} = H_{m,n} a_{m,n} + \underbrace{j \sum_{\substack{(p,q)\in\Omega \\ (p,q)\neq(m,n)}} H_{p,q} a_{p,q} \langle g \rangle_{m,n}^{p,q}}_{U_{p,q}} + w_{m,n}, \tag{4}$$

where $\langle g \rangle_{m,n}^{p,q} = \sum_{l=0}^{KN-1} g_{m,n}(l)\, g_{p,q}^*(l)$, $H_{m,n}$ is the channel frequency response, $U_{p,q}$ and $w_{m,n}$ are the associated interference and noise components, respectively. The channel frequency response is almost constant over the neighborhood.

TABLE 1. Intrinsic interference of $a_{m,n} = 1$ conveyed by the FBMC/OQAM transceiver.

	m-4	*m*-3	*m*-2	*m*-1	*m*	*m*+1	*m*+2	*m*+3	*m*+4
***n*-1**	0.0054	$0.0429j$	-0.1250	$-0.2058j$	0.2393	$0.2058j$	-0.1250	$-0.0429j$	0.0054
n	0	-0.0668	$0.0002j$	0.5644	1	0.5644	$0.0002j$	-0.0668	0
***n*+1**	0.0054	$-0.0429j$	-0.1250	$+0.2058j$	0.2393	$-0.2058j$	-0.1250	$0.0429j$	0.0054

Hence, equation (4) can be rewritten as

$$\hat{a}_{m,n} = H_{m,n}(a_{m,n} + j \underbrace{\sum_{\substack{(p,q)\in\Omega \\ (p,q)\neq(m,n)}} a_{p,q} \langle g \rangle_{m,n}^{p,q}}_{u_{p,q}}) + w_{m,n}. \quad (5)$$

Unfortunately, $\langle g \rangle_{m,n}^{p,q} \neq \delta_{m,p}\delta_{n,q}$, which means there is intrinsic interference in the FBMC/OQAM system. Specifically, the intrinsic interference of $a_{m,n} = 1$ conveyed by the transceiver of FBMC/OQAM is illustrated in Table I, where the prototype filter used is derived from [3]. Fortunately, when $a_{m,n}$ is a real symbol, $a_{m-1,n}, a_{m+1,n}, a_{m,n-1}$ and $a_{m,n+1}$ are imaginary symbols. Therefore, the intrinsic interference can be avoided, which is the so-called OQAM. However, due to the intrinsic interference, the conventional channel estimation and MIMO schemes used in OFDM systems cannot be directly applied to FBMC/OQAM.

III. FBMC/QAM TRANSCEIVER ARCHITECTURE

In this section, we present a new FBMC/QAM transceiver architecture. According to this scheme, a model that is more suitable for short package transmission is also proposed. Moreover, the impact of different pulse shaping filters on the BER performance is also compared.

A. FBMC/QAM AND CS-FBMC/QAM TRANSMITTER

The input of FBMC/QAM is a complex-valued QAM matrix $\mathbf{D} = \{d_{m,n}\}_{M\times N}$. The elements of $\mathbf{D}$ correspond to a time-frequency grid, where $d_{m,n}$ denotes the data transmitted on the nth sub-carrier during the mth symbol time, N is the total number of sub-carriers, and M is the number of symbols. Then, $\mathbf{D}$ is reshaped by parallel-to-serial conversion to a sequence

$$\mathbf{d} = \{d_k\}_{MN\times 1}, \quad (6)$$

where $k = 0, 1, \ldots, MN-1, k \in \mathbb{Z}$.

Similar to OFDM, the upconversion of the sub-carriers can be realized through the Inverse Discrete Fourier Transform (IDFT). This operation corresponds to a multiplication with the IDFT matrix. However, in order to reduce the large side-lobe levels resulting from the rectangular pulse of OFDM, any schemes of FBMC, including FBMC/QAM, utilizes well-designed pulse shapes. The combination of the IDFT matrix and the prototype filter can be expressed as

$$\mathbf{W} = \left\{w^{l,n}\right\} = \begin{bmatrix} w^{0,0} & \cdots & w^{0,N-1} \\ \vdots & \ddots & \vdots \\ w^{KN-1,0} & \cdots & w^{KN-1,N-1} \end{bmatrix}, \quad (7)$$

where W is a $KN \times N$ matrix, $w^{l,n} = \frac{1}{\sqrt{KN}} e^{\frac{j2\pi nl}{N}} g(l)$, l represents the sample index ($l = 0, 1, \ldots, KN-1, l \in \mathbb{Z}$). The sub-carrier spacing is $1/N$. K is the upsample factor, and generally $K = 4$. Conventional FBMC uses OQAM to transmit the real and imaginary parts of complex-valued symbols, and the real or imaginary part is delayed by half the symbol duration. However, the proposed scheme of FBMC directly uses QAM, hence contiguous symbols partially overlap one another with N as shown in Fig. 1. Therefore, the overlap and sum structure of the matrix can be composed of $\mathbf{W}$ as illustrated in Fig. 2.

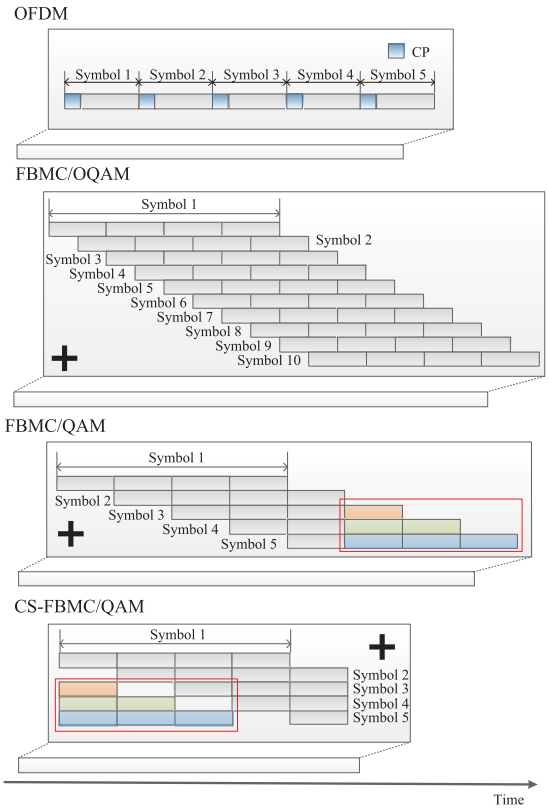

FIGURE 1. The length of symbols in time-domain.

The output of the transmitter in the FBMC/QAM system can be carried over to the more convenient form as follows

$$\mathbf{s} = \mathbf{G}\mathbf{d}, \quad (8)$$

where $\mathbf{G}$ is the transmitter matrix of the FBMC/QAM scheme. This expression for generating the transmit signal allows applying standard receive methods. Moreover, with respect to implementation, the transmitter is just a matrix

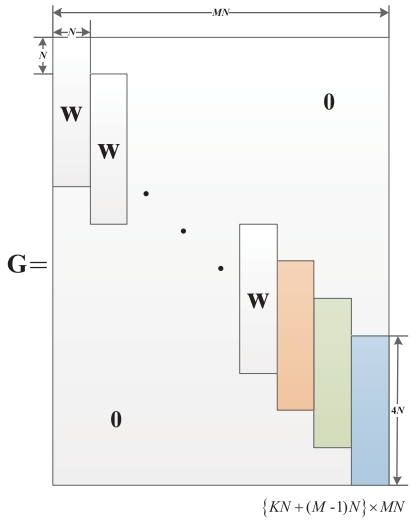

FIGURE 2. Matrix structure for the transmitter in the FBMC/QAM transceiver.

multiplication. Hence, a benefit of the new transceiver of FBMC/QAM is that scaling the matrix or using different precomputed matrices is an easy way to adapt the transmit signal to different frequency bands. The transmitter of the proposed FBMC/QAM scheme also can be expressed as

$$\begin{aligned} s(l) &= \sum_{m=0}^{M-1}\sum_{n=0}^{N-1} a_{m,n} g_{m,n}(l) \\ &= \sum_{m=0}^{M-1}\sum_{n=0}^{N-1} a_{m,n} e^{j\frac{2\pi nl}{N}} g(l - mN), \end{aligned} \tag{9}$$

where $l \in \mathbb{Z}$ is the sample index, $a_{m,n}$ denotes a complex-valued QAM symbol. This means that FBMC/QAM can select arbitrary QAM symbols like OFDM rather than only using the real or imaginary symbol like FBMC/OQAM. Of particular note is that the symbol rate of the FBMC system which transmits QAM symbols is the same as CP-OFDM. However, the time domain symbol length of FBMC/QAM is much longer than that of OFDM, which is not suitable for short package transmission.

In order to reduce the time domain symbol length of FBMC/QAM scheme, a CS-FBMC/QAM scheme is also proposed, which is a different form of FBMC/QAM. Cycle superimposition can also be implemented by a matrix, and the final constructed matrix is shown in Fig. 3.

The output of the transmitter in the CS-FBMC/QAM matrix scheme is given by [25]

$$\mathbf{s} = \tilde{\mathbf{G}}\mathbf{d}, \tag{10}$$

where $\tilde{\mathbf{G}}$ is the transmitter matrix of the CS-FBMC/QAM scheme. The benefits of the CS-FBMC/QAM matrix scheme lie that the transmission time domain signal is shorter than the CP-OFDM systems. Hence, the CS-FBMC/QAM matrix scheme is more suitable for short package transmission.

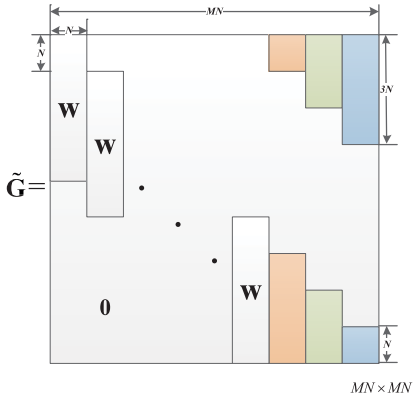

FIGURE 3. Transmitter matrix model for the CS-FBMC/QAM scheme.

B. RECEIVER

1) MATCHED FILTER RECEIVER

One way to receive the FBMC/QAM signal is to apply a matched filter on each sub-carrier separately. The main disadvantage of the MF receiver is that the ISI and ICI resulting from non-orthogonal pulse shapes can severely deteriorate the BER performance. As the received signal is arranged into a vector, the matched-filter receiver is described as follows

$$\hat{\mathbf{d}} = \mathbf{G}^H \mathbf{r}, \tag{11}$$

where $(\cdot)^H$ denotes Hermitian conjugate.

2) ZERO FORCING RECEIVER

Another method is the ZF receiver, which uses the inverse transmission matrix to mitigate the ISI and ICI. The ZF receiver can be described as

$$\hat{\mathbf{d}} = \mathbf{G}^{+}\mathbf{r}, \tag{12}$$

where $\mathbf{G}^{+} = \left(\mathbf{G}^H\mathbf{G}\right)^{-1}\mathbf{G}^H$. However, it also gathers noise from outside the band of interest, which results in noise enhancement.

3) MINIMUM MEAN SQUARE ERROR RECEIVER

A major drawback of the ZF receiver is that the noise might be amplified. This weakness is addressed by the minimum mean square error (MMSE) receiver

$$\hat{\mathbf{d}} = \mathbf{G}^{\dagger}\mathbf{r}, \tag{13}$$

$$\mathbf{G}^{\dagger} = \left(\frac{\sigma_{\mathbf{n}}^2}{\sigma_{\mathbf{d}}^2}\mathbf{I} + \mathbf{G}^H\mathbf{G}\right)^{-1}\mathbf{G}^H. \tag{14}$$

C. CONDITION NUMBER

Thanks to matrix theory, it can be seen from (8) that if the condition number of matrix $\mathbf{G}$ is large, the numerical stability is poor. That is, a slight change in $\mathbf{s}$ may cause a great change in $\mathbf{d}$. However, if the condition number of matrix $\mathbf{G}$ is small, the numerical stability is good. That is, a slight change in $\mathbf{s}$ only cause a small change in $\mathbf{d}$. Therefore, the condition

TABLE 2. Condition number.

Filter type	PHYDYAS in [3]	SRRC (roll-off factor r=0.1)
Condition number	6.6966	2.6535

number of matrix $\mathbf{G}$ can be used as a criterion for selecting the filter.

After the singular value decomposition of matrix $\mathbf{G}$, the singular value matrix is obtained. Taking out the maximum singular value and the smallest singular value in matrix $\mathbf{G}$, the ratio of the two value is defined as the condition number. Actually, the condition number indicates the sensitivity of calculation to errors. As can be seen from Table II, the condition number of the PHYDYAS filter and the square root raised cosine (SRRC) filter are 6.6966 and 2.6535, respectively. Therefore, from the perspective of condition number, it can be predicted that the receiving performance of the SRRC filter is better than that of the PHYDYAS filter.

IV. CHANNEL ESTIMATION FOR FBMC/QAM SCHEME

In this section, our purpose is to verify whether the proposed FBMC/QAM matrix scheme can use the same channel estimation technique used in conventional OFDM systems. Fig. 4 describes the pilot positions in seven symbols.

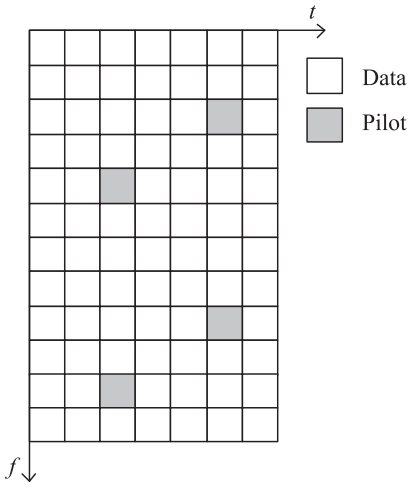

FIGURE 4. Pilot positions of per RB in seven symbols.

A. IDEAL CHANNEL ESTIMATION

In OFDM systems, after removing the CP, the output signal of the channel can be expressed as

$$r(n) = s(n) \otimes h(n) + w(n), \tag{15}$$

where $\otimes$ denotes circular convolution. In the frequency domain, equation (16) can be written as follows

$$R = SH + W, \tag{16}$$

where H and W are the DFT of $h(n)$ and $w(n)$ in (16), respectively.

For ideal channel estimation, the channel characteristics H in the frequency domain are well known at the receiver side. Consequently, after FDE, the OFDM frequency signal can be expressed as

$$\bar{S} = \frac{R}{H} = S + \bar{W}, \tag{17}$$

where $\bar{W} = W/H$.

In the FBMC/OQAM system, equation (5) can be rewritten as

$$\hat{a}_{m,n} = H_{m,n}(a_{m,n} + ju_{p,q}) + w_{m,n}. \tag{18}$$

The intrinsic interference $ju_{p,q}$ is the imaginary part from the neighboring symbols and sub-carriers. Therefore, we can select the real field to obtain the accurate demodulated signal after FDE.

In the FBMC/QAM scheme, after MF detector, the output signal can be described as

$$\hat{d}_{m,n} = H_{m,n}d_{m,n} + \underbrace{\sum_{\substack{(p,q)\in\Omega \\ (p,q)\neq(m,n)}} H_{p,q}d_{p,q}\langle g\rangle_{m,n}^{p,q}}_{I_{p,q}} + w_{m,n}. \tag{19}$$

It can be seen that the intrinsic interference $I_{p,q}$ cannot be eliminated by the MF receiver. Therefore, the ZF or MMSE receiver needs to be employed to eliminate the intrinsic interference.

B. LS CHANNEL ESTIMATION

The optimality criterion of the least squares (LS) method is to minimize the least square errors to find an optimal estimator for the unknown parameters. The normalized value can be written as

$$H_{LS} = \arg\min\left\{\left(\hat{d} - Hd\right)^H\left(\hat{d} - Hd\right)\right\}. \tag{20}$$

The channel coefficient of FBMC/QAM using LS estimation at pilot positions can be obtained as follows

$$H_{LS_p} = \frac{\hat{d}_p}{d_p}, \tag{21}$$

where $\hat{d}_p$ and d_p denote the pilot position in $\hat{d}$ and d, respectively. Thus using interpolation methods can obtain the whole channel characteristics H_{LS}. Since the intrinsic interference can be eliminated by the ZF or MMSE receiver, a nearly accurate channel coefficient can be obtained.

However, when OQAM demodulation is applied in the FBMC/OQAM system, the channel coefficient $H_{m,n}$ is destroyed by selecting the real field. Therefore, it is difficult to implement real channel estimation in the conventional FBMC/OQAM system due to OQAM.

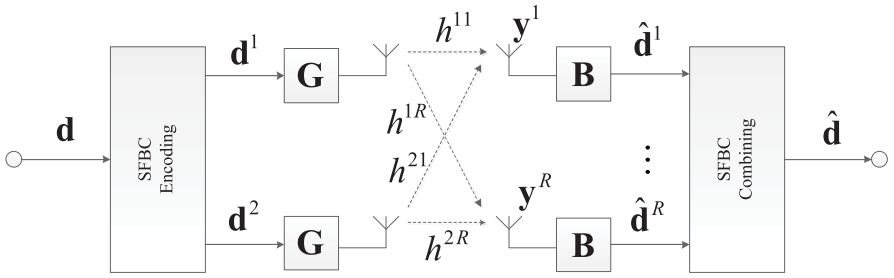

FIGURE 5. Block diagram of the MIMO FBMC system with Alamouti SFBC.

V. SPACE-FREQUENCY BLOCK CODING FOR FBMC/QAM SCHEME

The simplified block diagram for MIMO FBMC systems with Alamuoti SFBC is shown in Fig. 5. The transmit data $\mathbf{d}$ from (6) is firstly applied to SFBC encoding. Then, the output signals $\mathbf{d}^1$ and $\mathbf{d}^2$ for the first and second transmit antenna are defined as follows

$$\mathbf{d} = [d_1, d_2, \cdots, d_{MN}]^T, \tag{22}$$

$$\mathbf{d}^1 = \left[d_1, -d_2^*, \cdots, d_i, -d_{i+1}^*, \cdots, d_{MN-1}, -d_{MN}^*\right]^T, \tag{23}$$

$$\mathbf{d}^2 = \left[d_2, d_1^*, \cdots, d_{i+1}, d_i^*, \cdots, d_{MN}, d_{MN-1}^*\right]^T, \tag{24}$$

where $i = 1, 3, \cdots, MN-1$. The two data $\mathbf{d}^1$ and $\mathbf{d}^2$ are modulated with the FBMC/QAM transmitter independently. Therefore, the receive signal $\mathbf{y}^r$ at receiver antenna r is written as

$$\mathbf{y}^r = \mathbf{H}^{1r}\mathbf{G}\mathbf{d}^1 + \mathbf{H}^{2r}\mathbf{G}\mathbf{d}^2 + \mathbf{w}^r, \tag{25}$$

where $\mathbf{H}^{tr}$ is the channel convolution matrix from the transmit antenna t to receive antenna r.

At the receiver side, before SFBC combining, the signal on each of the R receiver antenna is demodulated by matrix $\mathbf{B}$

$$\hat{\mathbf{d}}^r = \mathbf{B}\mathbf{y}^r = H^{1r}\mathbf{d}^1 + H^{2r}\mathbf{d}^2 + \bar{\mathbf{w}}^r, \tag{26}$$

where H^{tr} denotes the DFT of the channel impulse response h^{tr}, $\mathbf{B}$ is the receiver matrix, which can be the MF, ZF or MMSE matrix. For ease of exposition, we regard $\mathbf{B} = \left(\mathbf{G}^H\mathbf{G}\right)^{-1}\mathbf{G}^H$ as the ZF receiver matrix. Equation (28) can also be described in detail as follows

$$\hat{d}_i^r = H_i^{1r} d_i + H_i^{2r} d_{i+1} + \bar{w}_i^r, \tag{27}$$

$$\hat{d}_{i+1}^r = H_{i+1}^{1r}(-d_{i+1}^*) + H_{i+1}^{2r} d_i^* + \bar{w}_{i+1}^r, \tag{28}$$

where H_i^{tr} denotes the ith point of the DFT of the channel impulse response h^{tr}, and $\hat{d}_i^r$ is the ith point of the $\hat{\mathbf{d}}^r$ on the receiver antenna r. Therefore, the SFBC combining is carried out separately according to the following rule

$$d_i = \frac{\sum_{r=1}^{R}(H_i^{1r})^*\hat{d}_i^r + H_i^{2r}(\hat{d}_{i+1}^r)^*}{\sum_{r=1}^{R}\left|H_i^{1r}\right|^2 + \left|H_i^{2r}\right|^2} + \tilde{w}_i, \tag{29}$$

$$d_{i+1} = \frac{\sum_{r=1}^{R}(H_i^{2r})^*\hat{d}_i^r - H_i^{1r}(\hat{d}_{i+1}^r)^*}{\sum_{r=1}^{R}\left|H_i^{1r}\right|^2 + \left|H_i^{2r}\right|^2} + \tilde{w}_{i+1}. \tag{30}$$

VI. LOW COMPLEXITY IMPLEMENTATION OF THE TWO PROPOSED FBMC/QAM SCHEME

Since intrinsic interference cannot be eliminated by the MF receiver, and the MMSE receiver has an impractical complexity, this section investigates a low-complexity implementation of the ZF receiver.

A. FBMC/QAM LOW COMPLEXITY IMPLEMENTATION

As shown in (12), the ZF receiver can be rewritten as

$$\hat{\mathbf{d}} = \left(\mathbf{G}^H\mathbf{G}\right)^{-1}\mathbf{G}^H\mathbf{r}. \tag{31}$$

We define that $\mathbf{B} = \left(\mathbf{G}^H\mathbf{G}\right)^{-1}$ and $\mathbf{P} = \mathbf{G}^H\mathbf{r}$. Then, (31) can be regard as

$$\hat{\mathbf{d}} = \mathbf{B} \cdot \mathbf{P}, \tag{32}$$

where $\hat{\mathbf{d}} = \left[\hat{\mathbf{d}}_1\hat{\mathbf{d}}_2\cdots\hat{\mathbf{d}}_M\right]^T$, $\mathbf{P} = [\mathbf{P}_1\mathbf{P}_2\cdots\mathbf{P}_M]^T$. $\mathbf{B}$ is an $MN \times MN$ symmetric matrix as follows

$$\mathbf{B} = \begin{bmatrix} \mathbf{C}_{1,1} & \mathbf{C}_{1,2} & \cdots & \mathbf{C}_{1,M} \\ \mathbf{C}_{2,1} & \mathbf{C}_{2,2} & \cdots & \mathbf{C}_{2,M} \\ \vdots & \vdots & \ddots & \vdots \\ \mathbf{C}_{M,1} & \mathbf{C}_{M,2} & \cdots & \mathbf{C}_{M,M} \end{bmatrix}, \tag{33}$$

where $\mathbf{C}_{i,j} = \mathbf{C}_{j,i} \quad i,j = 1, \cdots, M$, and $\mathbf{C}_{i,j}$ is an $N \times N$ circulant matrix

$$\mathbf{C}_{i,j} = \begin{bmatrix} c_1 & c_n & \cdots & c_2 \\ c_2 & c_1 & \cdots & c_3 \\ \vdots & \vdots & \ddots & \vdots \\ c_n & c_{n-1} & \cdots & c_1 \end{bmatrix}. \tag{34}$$

All circulant matrices can made diagonal through the use of the DFT. Therefore, $\mathbf{C}_{i,j}$ can be expressed as

$$\mathbf{C}_{i,j} = \mathcal{F}^{-\infty}\Lambda_{i,j}\mathcal{F}, \tag{35}$$

where $\mathcal{F}^{-\infty}$ and $\mathcal{F}$ represent the IDFT and DFT, respectively. $\Lambda_{i,j} = diag\left(\hat{v}_{i,j}\right)$ and $\hat{v}_{i,j}$ is the DFT of the first column of $\mathbf{C}_{i,j}$. Then, $\hat{\mathbf{d}}_i$ from $\hat{\mathbf{d}}$ can be calculated by the following equation

$$\hat{\mathbf{d}}_i = \sum_{j=1}^{M}\mathbf{C}_{i,j}\mathbf{P}_j = \sum_{j=1}^{M}F^{-1}\Lambda_{i,j}F\mathbf{P}_j, \tag{36}$$

where $i, j = 1, 2, \cdots, M$. The detailed diagram of the FBMC/QAM-ZF low complexity receiver is shown in Fig. 6.

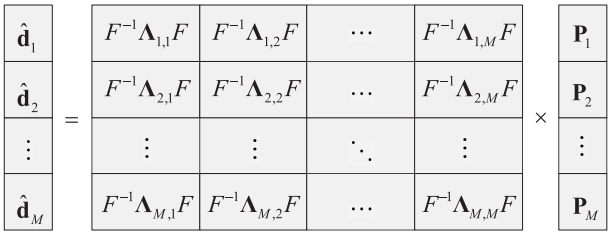

FIGURE 6. Diagram of the FBMC/QAM-ZF low complexity receiver.

B. CS-FBMC/QAM LOW COMPLEXITY IMPLEMENTATION

In this section, we study on the low complexity implementation of the CS-FBMC/QAM matrix scheme [26]. Without loss of generality, the received signal can be simplified as

$$\mathbf{r} = \tilde{\mathbf{G}}\mathbf{d} + \mathbf{w}. \tag{37}$$

Then the DFT is applied on both sides of (37). Hence, the above equation can be expressed as

$$\mathcal{F}_{MN}\mathbf{r} = \mathcal{F}_{MN}\tilde{\mathbf{G}}\mathcal{F}_{MN}^{-1}\mathcal{F}_{MN}\mathbf{d} + \mathcal{F}_{MN}\mathbf{w}. \tag{38}$$

Let $\mathbf{B} = \mathcal{F}_{MN}\tilde{\mathbf{G}}\mathcal{F}_{MN}^{-1}$, equation (38) can be rewritten as

$$\bar{\mathbf{r}} = \mathbf{B}\bar{\mathbf{d}} + \bar{\mathbf{w}}, \tag{39}$$

where $\bar{\mathbf{r}}$, $\bar{\mathbf{d}}$ and $\bar{\mathbf{w}}$ denote the frequency signals of $\mathbf{r}$, $\mathbf{d}$ and $\mathbf{w}$, respectively.

It is found that $\mathbf{B}$ has the following characteristics: $\mathbf{B} = \left[\mathbf{B}^{(1)}\mathbf{B}^{(2)}\cdots\mathbf{B}^{(N)}\right]$, where

$$\mathbf{B}^{(n)} = \begin{bmatrix} b_1^{(n)} & 0 & \cdots & 0 \\ 0 & b_2^{(n)} & \cdots & 0 \\ \vdots & \vdots & \ddots & \vdots \\ 0 & 0 & \cdots & b_M^{(n)} \\ & \vdots & & \\ b_{(N-1)M+1}^{(n)} & 0 & \cdots & 0 \\ 0 & b_{(N-1)M+2}^{(n)} & \cdots & 0 \\ \vdots & \vdots & \ddots & \ddots \\ 0 & 0 & \cdots & b_{NM}^{(n)} \end{bmatrix} \tag{40}$$

According to the structure of $\mathbf{B}$, one can obtain a diagonal block matrix by rearranging rows and columns. The specific arrangement is as follows. TakE a row in every M rows and select one in every M column, then pile them together. The resulting diagonal block matrix $\tilde{\mathbf{B}}$ is as follows

$$\tilde{\mathbf{B}} = \begin{bmatrix} \tilde{\mathbf{B}}_1 & & & \\ & \tilde{\mathbf{B}}_2 & & \\ & & \ddots & \\ & & & \tilde{\mathbf{B}}_M \end{bmatrix}_{MN\times MN}, \tag{41}$$

TABLE 3. Simulation parameters for the proposed FBMC/QAM scheme.

Parameter	Value	
	OFDM	FBMC
Modulation	QPSK, 64QAM	
Samples per symbol N	128	128
Number of active sub-carriers N_{on}	36	36
Block size (symbols) M	7	7
Sub-carrier spacing (kHz)	15	15
CP length (samples) L_{cp}	9	9
Shaping pulse	Rectangular	SRRC
Roll-off factor r	-	0.1
Channel model h_n	AWGN, PB	
PB delay (ns)	[0 200 800 1200 2300 3700]	
PB power (dB)	[0 -0.9 -4.9 -8.0 -7.8 -23.9]	
Channel coding	Turbo code	
Pilot spacing (sub-carriers)	6	6
Estimation algorithm	Ideal/LS	

where $\tilde{\mathbf{B}}_m$ is an $N \times N$ matrix. The structure of $\tilde{\mathbf{B}}_m$ is represented as follows

$$\tilde{\mathbf{B}}_m = \begin{bmatrix} b_m^{(1)} & b_m^{(2)} & \cdots & b_m^{(N)} \\ b_{M+m}^{(1)} & b_{M+m}^{(2)} & \cdots & b_{M+m}^{(N)} \\ \vdots & \vdots & \ddots & \vdots \\ b_{(N-1)M+m}^{(1)} & b_{(N-1)M+m}^{(2)} & \cdots & b_{(N-1)M+m}^{(N)} \end{bmatrix}. \tag{42}$$

In order to ensure equality of both sides of the equation, $\bar{\mathbf{r}}$ and $\bar{\mathbf{w}}$ also perform the same row arrangement as $\mathbf{B}$ to obtain $\tilde{\mathbf{r}}$ and $\tilde{\mathbf{w}}$. $\bar{\mathbf{d}}$ also performs the same column arrangement as $\mathbf{B}$, to obtain $\tilde{\mathbf{d}}$. Thus, the arranged expression can be written as

$$\tilde{\mathbf{r}} = \tilde{\mathbf{B}}\tilde{\mathbf{d}} + \tilde{\mathbf{w}}. \tag{43}$$

Since $\tilde{\mathbf{B}}$ is a diagonal block matrix, each of the sub-block can be solved independently. Therefore, equation (43) can be broken down into

$$\tilde{\mathbf{r}}_m = \tilde{\mathbf{B}}_m\tilde{\mathbf{d}}_m + \tilde{\mathbf{w}}_m. \tag{44}$$

Thus the receiver can divide the data into small pieces to obtain the signal

$$\tilde{\mathbf{d}}_m' = \mathbf{Q}\tilde{\mathbf{r}}_m + \mathbf{Q}\tilde{\mathbf{w}}_m, \tag{45}$$

where $\mathbf{Q}$ is the receiver matrix. In order to recover the desired signal, it is necessary to take a column in every M columns of $\tilde{\mathbf{d}}'$ to get $\bar{\mathbf{d}}'$. Then, the final signal $\mathbf{d}'$ can be obtained after the IDFT.

VII. SIMULATION RESULTS

In this section, we compare the BER performance of the proposed FBMC/QAM and CS-FBMC/QAM matrix scheme with those of the conventional FBMC/OQAM and OFDM systems. The detailed simulation parameters are listed in Table III.

A. POWER SPECTRAL DENSITIES OF OFDM, FBMC/QAM AND CS-FBMC/QAM

Fig. 7 compares the power spectral density (PSD) of the proposed FBMC/QAM, CS-FBMC/QAM and OFDM systems.

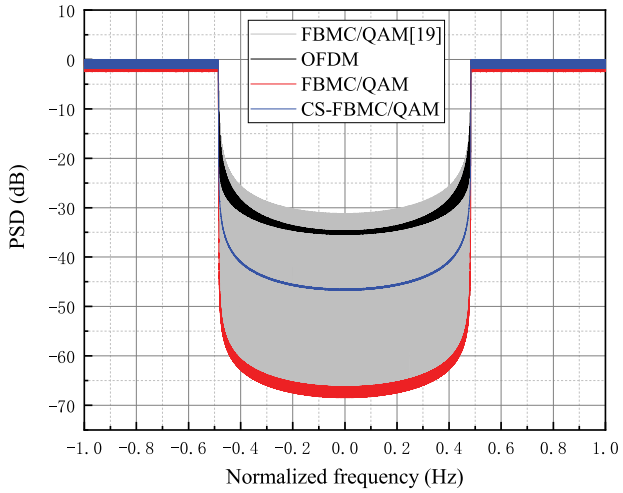

FIGURE 7. PSD comparison between OFDM, FBMC/QAM and CS-FBMC/QAM.

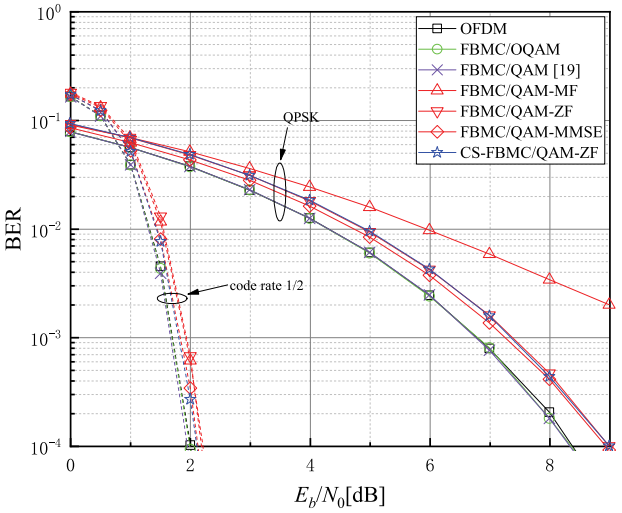

FIGURE 9. BER performance of our proposed FBMC/QAM matrix scheme using the SRRC filter compared with the FBMC/OQAM and OFDM for $N = 128$, $M = 7$ in the AWGN channel.

It can be seen that the proposed FBMC/QAM scheme has the lowest OOB emissions. As the time domain symbol of CS-FBMC/QAM is superposed by cycle, the OOB emissions of CS-FBMC/QAM is higher than that of FBMC/QAM, but it is still better than those of OFDM and FBMC/QAM in [19]. OFDM uses the rectangular pulse shape to yield higher OOB emissions. FBMC/QAM in [19] utilizes two filters on odd and even numbered sub-carriers. However, due to the abrupt changes in the odd filter, the OOB emissions becomes very high.

B. PERFORMANCE COMPARISON IN AWGN CHANNEL

As can be seen from Fig. 8, the BER performance of the proposed FBMC/QAM and CS-FBMC/QAM matrix scheme using the PHYAYDS filter is worse than that of OFDM and FBMC/OQAM system in the AWGN channel [27]. This is due mainly to the choice of the filter. When a PHYAYDS filter is applied, serious intrinsic interference is experienced, which is hard to eliminate by the ZF or MMSE receiver only. FBMC/QAM in [19] can also achieve the same BER performance compared with OFDM, since the interference between adjacent carriers is eliminated. The Turbo coded BER performance also shows that the FBMC/QAM and CS-FBMC/QAM matrix scheme cannot demodulate the similar results as OFDM due to the effect of self-interference.

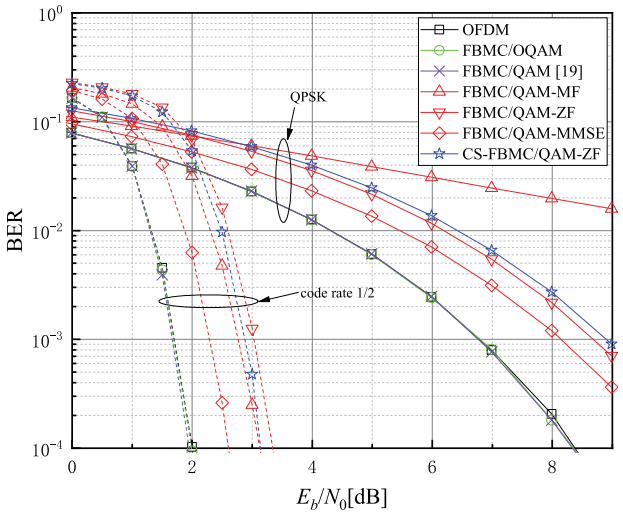

FIGURE 8. BER performance of the proposed FBMC/QAM scheme using the PHYAYDS filter compared with the FBMC/OQAM and OFDM for $N = 128$, $M = 7$ in the AWGN channel.

However, it can be seen from Fig. 9 that the performance of the proposed FBMC/QAM and CS-FBMC/QAM matrix scheme is much better than that of Fig. 8. The simulation results are consistent with the conclusion of the condition number in Section III. The Turbo coded BER performance of FBMC/QAM and CS-FBMC/QAM matrix scheme is almost the same as OFDM systems.

C. PERFORMANCE COMPARISON IN PB CHANNEL

In the previous subsection, It is proved that the performance of the SRRC filter is better than that of the PHYAYDS filter in FBMC/QAM and CS-FBMC/QAM matrix scheme. Therefore, only SRRC filter is used in the following simulations [28].

1) IDEAL CHANNEL ESTIMATION

Fig. 10 depicts the BER performance of the proposed FBMC/QAM and CS-FBMC/QAM matrix scheme in the PB channel with ideal estimation. It can be seen that the FBMC/OQAM system can achieve the same BER performance as the OFDM system, since the channel characteristics are well known at the receiver side [29]. When in the high SNR region, the performance of FBMC/QAM in [19] is worse than that of OFDM. The proposed FBMC/QAM and CS-FBMC/QAM matrix scheme suffer from intrinsic

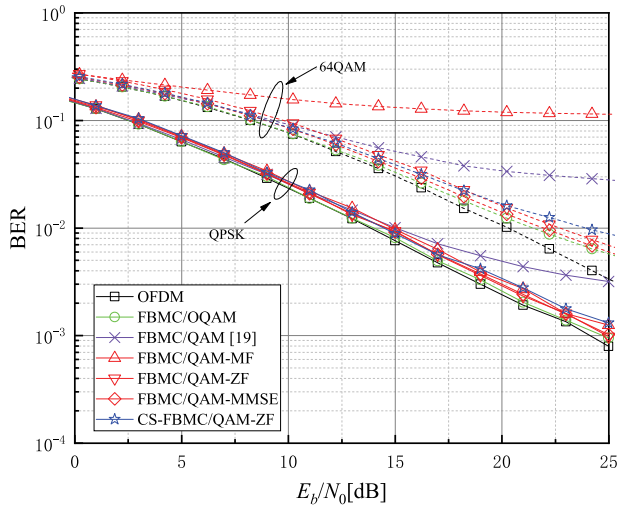

FIGURE 10. BER performance of the proposed FBMC/QAM matrix scheme using the SRRC filter compared with the FBMC/OQAM and OFDM for $N = 128$, $M = 7$ in the PB channel with ideal estimation.

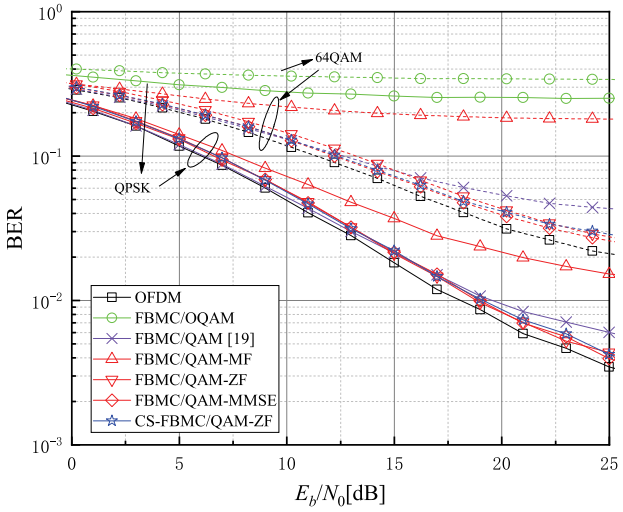

FIGURE 11. BER performance of the proposed FBMC/QAM matrix scheme using the SRRC filter compared with the FBMC/OQAM and OFDM for $N = 128$, $M = 7$ in the PB channel with LS estimation.

interference because of the use of the QAM symbol. However, the intrinsic interference is not the predominant factor when passing through the multi-path fading channel. Therefore, the proposed FBMC/QAM and CS-FBMC/QAM matrix scheme can still achieve almost the same BER performance when compared with the OFDM systems. When 64QAM modulation is employed, the BER performances of all the FBMC scheme slightly deviate from OFDM at high SNRs, especially the MF receiver. Obviously, this is also due to the effect of the intrinsic interference.

2) LS CHANNEL ESTIMATION

When ZF or MMSE receiver is used, the proposed FBMC/QAM CS-FBMC/QAM matrix scheme in Fig. 11 can almost achieve the same BER performance compared with OFDM systems. The performance of FBMC/QAM with MF receiver becomes worse due to the intrinsic interference. The performance of FBMC/QAM in [19] is still worse in the high SNR region. The FBMC/OQAM system has the worst BER performance because FBMC/OQAM cannot estimate the channel coefficient correctly without the use of other means.

3) MSE OF LS CHANNEL ESTIMATION

Fig. 12 illustrates the MSE of LS channel estimation for the proposed FBMC/QAM and CS-FBMC/QAM matrix scheme over the PB channel. The results show that the FBMC/OQAM receiver is unable to completely estimate the channel characteristic. As FBMC/OQAM is a real orthogonal system, which needs to transmit the real and imaginary parts of complex-valued symbols. However, the channel coefficient is destroyed by selecting the real field. When in the high SNR region, self-interference becomes the main interference. Therefore, the channel estimation performance of FBMC/QAM-MF receiver is worse than that of OFDM systems, since the FBMC/QAM-MF receiver has no counter-measures for self-interference. The FBMC/QAM-ZF, FBMC/QAM-MMSE, CS-FBMC/QAM-ZF and FBMC/QAM in [19] can mitigate self-interference. Thus, the channel estimation of these receivers can almost achieve the same MSE performance compared with OFDM systems.

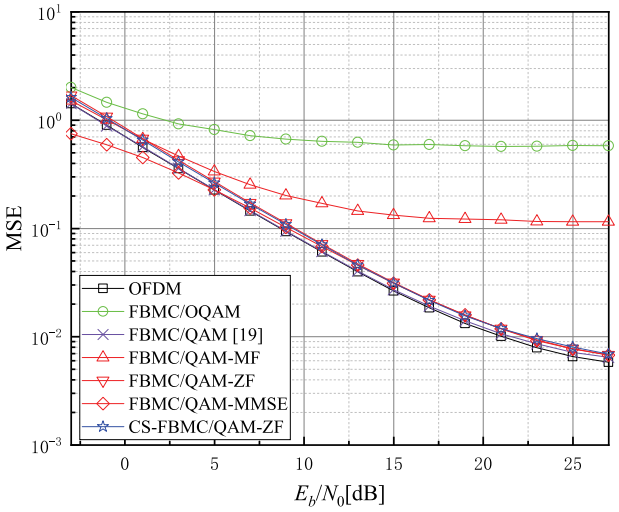

FIGURE 12. MSE performance comparison of channel estimation in the PB channel.

D. PERFORMANCE COMPARISON OF SFBC FOR FBMC/QAM SCHEME

It is possible to observe from Fig. 13 that SFBC-FBMC/OQAM still cannot get the correct result even using ideal estimation. As SFBC encoding and combining requires conjugate operations, which breaks the characteristics of intrinsic interference in the SFBC-FBMC/OQAM

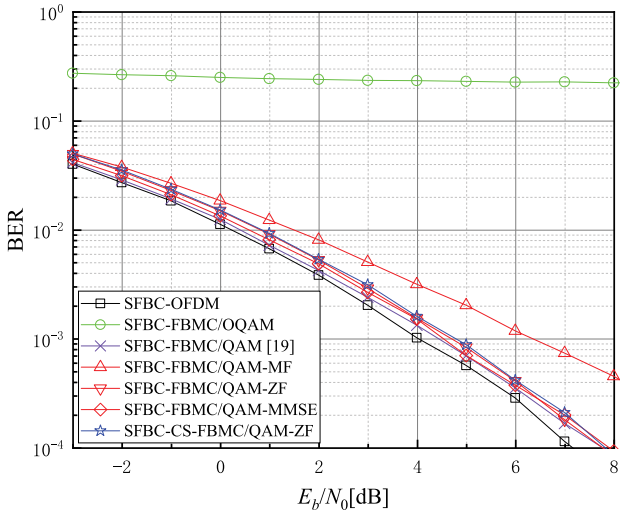

FIGURE 13. BER performance of the proposed SFBC-FBMC/QAM scheme using the SRRC filter compared with the FBMC/OQAM and OFDM for $N = 128$, $M = 7$ in the PB channel with ideal estimation.

TABLE 4. Computational complexity of different FBMC receiver techniques.

Techniques	Number of Complex Multiplications
OFDM	$\frac{1}{2}MN\log_2(N)$
FBMC-OQAM	$2M\left(\frac{1}{2}N\log_2(N)+KN\right)$
FBMC-MF	$MN(KN+(M-1)N)$
FBMC-ZF	$MN(KN+(M-1)N)$
FBMC-ZF-Low	$\frac{3}{2}MN\log_2(N)+KN+MN$
CS-FBMC/QAM-MF	M^2N^2
CS-FBMC/QAM-ZF	M^2N^2
CS-FBMC/QAM-Low	$MN\log_2(MN)+MN^2$
FBMC/QAM [19]	$2M\left(\frac{1}{2}KN\log_2(KN)+KN\right)$

system. Consequently, SFBC-FBMC/OQAM cannot effectively use OQAM to eliminate the intrinsic interference. The performance of SFBC-FBMC/QAM in [19] is similar to that of the proposed SFBC-FBMC/QAM-ZF. As the SNR increases, the BER performance of the SFBC-FBMC/QAM-MF scheme decreases relative to the SFBC-OFDM system, because the SFBC-FBMC/QAM-MF receiver does not have any counter-measures to self-interference. The SFBC-FBMC/QAM-ZF and SFBC-CS-FBMC/QAM-ZF receiver can mitigate the self-interference. However, in the high SNR region, the enhanced noise also leads to performance degradation relative to SFBC-OFDM. The SFBC-FBMC/QAM-MMSE receiver has the best BER performance in the proposed FBMC/QAM scheme, since the MMSE receiver is designed in consideration of both self-interference and noise.

E. COMPLEXITY ANALYSIS

Table 4 describes the computational complexity of different FBMC receivers. The complexity analysis is based on the number of complex multiplications (CMs). A total number of N sub-carriers and M symbols are considered.

Techniques	Number of Complex Multiplications
OFDM	$\frac{1}{2}MN\log_2(N)$
FBMC-OQAM	$2M\left(\frac{1}{2}N\log_2(N)+KN\right)$
FBMC-MF	$MN(KN+(M-1)N)$
FBMC-ZF	$MN(KN+(M-1)N)$
FBMC-ZF-Low	$\frac{3}{2}MN\log_2(N)+KN+MN$
CS-FBMC/QAM-MF	M^2N^2
CS-FBMC/QAM-ZF	M^2N^2
CS-FBMC/QAM-Low	$MN\log_2(MN)+MN^2$
FBMC/QAM [19]	$2M\left(\frac{1}{2}KN\log_2(KN)+KN\right)$

FIGURE 14. Computational complexity comparison of different FBMC receiver techniques and $N = 1024$ with respect to different values of M.

In OFDM, each N-point DFT requires $\frac{1}{2}N\log_2 N$ CMs. Accordingly, OFDM needs $\frac{1}{2}MN\log_2(N)$ CMs. In FBMC/OQAM, the receiver requires twice KN-point filter multiplication and N-point DFT in per symbol. Therefore, the receiver computational complexity $C_{FBMC/OQAM}$ can be calculated as $2M\left(\frac{1}{2}N\log_2(N)+KN\right)$. In the FBMC/QAM matrix scheme, due to the fact that the receiving matrices of MF and ZF can be stored in advance, thus they have the same computational complexity.

The FBMC/QAM-ZF-Low receiver can be divided into two parts according to (34). In the first part, the result of $\mathbf{P}$ can be regard as an MF receiver which can be obtained by the FBMC/QAM non-matrix scheme. The FBMC/QAM non-matrix scheme needs once KN-point filter multiplication and N-point DFT per symbol. Hence, the computational complexity of FBMC/QAM is $M\left(\frac{1}{2}N\log_2(N)+KN\right)$. The second part is described in (38). In each $F^{-1}\Lambda_{i,j}F\mathbf{P}_j$ the computational complexity is $N\log_2(N)+N$, there are $M\times M$ times of this operation in total. Therefore, the computational complexity of FBMC-ZF-Low is $\frac{3}{2}MN\log_2(N)+KN+MN$.

The matrix dimension of CS-FBMC/QAM-MF and CS-FBMC/QAM-ZF receiver is $MN\times MN$. Therefore, they all need M^2N^2 CMs. In the CS-FBMC/QAM-ZF-Low receiver, the receiving matrix is divided into M submatrices, which simplifies computation, and the number of CMs is $MN\log_2(MN)+MN^2$.

The computational complexity discussed above is evaluated and plotted in Fig. 14 for $N = 1024$ with respect to different values of M. Due to the fact that the complexity of the MMSE receiver with direct matrix inversion and multiplications is prohibitively high compared with other techniques, it is not presented in our comparison. As depicted in Fig. 14, the computational complexity of the proposed FBMC/QAM-ZF-Low is more than 100 times lower than those of FBMC/QAM-MF and FBMC/QAM-ZF, when the number of symbols M is small. Moreover, the computational complexity of the proposed FBMC/QAM-ZF-Low is also lower than that of FBMC/QAM in [19], when the number of symbols is less than 4. When $M = 1$, the complexity of FBMC/QAM-ZF-Low and FBMC/OQAM is basically the same. However, as the number of symbols M increase, the complexity of FBMC/QAM-ZF-Low becomes

higher than that of FBMC/OQAM, because the complexity of the second part of FBMC/QAM-ZF-Low is greatly affected by the number of symbols M. In the CS-FBMC/QAM-Low, the receiving matrix is divided into M submatrices. Therefore, the complexity of the CS-FBMC/QAM-Low is becomes lower and lower than the CS-FBMC/QAM-MF and CS-FBMC/QAM-ZF as M increases. Therefore, the low-complexity approach is more suitable for the situations where the number of symbols is large.

F. STORAGE ANALYSIS

In the proposed FBMC/QAM matrix scheme, The matrix dimensions of the ZF receiver $\mathbf{G}^{+}$ depends on the number of symbols and sub-carriers. With the increase of the number of symbols and sub-carriers, the matrix dimension becomes very large. Hence, it is necessary to optimize the storage of the receiving matrix.

As can be observed from (34), $\mathbf{P}$ is the result of the MF receiver which can be obtained by the FBMC/QAM non-matrix scheme. Therefore, it only needs to store a KN point filter at the receiver side. It can be seen from (35) and (36) that $\mathbf{B}$ is an $MN \times MN$ symmetric matrix, and $\mathbf{C}_{i,j}$ is an $N \times N$ circulant matrix. Therefore, it is only necessary to store the upper or lower triangular matrix of $\mathbf{B}$. Furthermore, each matrix $\mathbf{C}_{i,j}$ can be represented by its first column elements. Finally, the required storage space for matrix $\mathbf{B}$ is $\frac{(M+1)MN}{2}$. Hence, the total storage space of the low complexity the ZF receiver is $\frac{(M+1)MN}{2} + KN$. Compared with the ZF receive matrix, the ratio of required storage space is as follows

$$R = \frac{(M+1)M + 2K}{2M(KN + (M-1)N)}. \tag{46}$$

For example, when $M = 14, N = 1024, K = 4$, the storage space of the low-complexity ZF receiver is 4.47×10^{-4} times lower than that of the ZF receiver.

VIII. CONCLUSION

In this paper, a FBMC/QAM matrix model was proposed, which is able to transmit QAM symbols in the FBMC system. Based on the model, the CS-FBMC/QAM scheme was also proposed, which is more suitable for short package transmission. At the receiver, the ZF receiver was mainly selected to eliminate intrinsic self-interference. The BER performance of the proposed FBMC/QAM and CS-FBMC/QAM matrix scheme in conjunction with conventional channel estimation and MIMO techniques was also evaluated. Moreover, the low-complexity ZF receiver structure for the FBMC/QAM and CS-FBMC/QAM matrix scheme was designed, which is capable of effectively reducing the complexity of the ZF receiver. The simulation results demonstrated that the proposed FBMC/QAM and CS-FBMC/QAM matrix scheme works well with the conventional channel estimation and MIMO techniques. What's more, the two proposed matrix schemes both had lower OOB emissions than OFDM systems, which may have more advantages in asynchronous transmission. In the future work on FBMC/QAM matrix scheme, the asynchronous transmission performance will be evaluated. In addition, the combination of FBMC/QAM matrix scheme with non-orthogonal multiple access (NOMA) will also be investigated, especially in the case of asynchronous interference.

REFERENCES

[1] P. Banelli, S. Buzzi, G. Colavolpe, A. Modenini, F. Rusek, and A. Ugolini, "Modulation formats and waveforms for 5G networks: Who will be the heir of OFDM?: An overview of alternative modulation schemes for improved spectral efficiency," *IEEE Signal Process. Mag.*, vol. 31, no. 6, pp. 80–93, Nov. 2014.

[2] T. Hwang, C. Yang, G. Wu, S. Li, and G. Y. Li, "OFDM and its wireless applications: A survey," *IEEE Trans. Veh. Technol.*, vol. 58, no. 4, pp. 1673–1694, May 2009.

[3] M. Bellanger *et al.*, "FBMC physical layer: A primer," *PHYDYAS*, vol. 25, no. 4, pp. 7–10, 2010.

[4] B. Farhang-Boroujeny, "OFDM versus filter bank multicarrier," *IEEE Signal Process. Mag.*, vol. 28, no. 3, pp. 92–112, May 2011.

[5] F. Schaich, "Filterbank based multi carrier transmission (FBMC)—Evolving OFDM: FBMC in the context of WiMAX," in *Proc. Eur. Wireless Conf. (EW)*, Lucca, Italy, Apr. 2010, pp. 1051–1058.

[6] Y. Medjahdi, M. Terre, D. Le Ruyet, D. Roviras, and A. Dziri, "Performance analysis in the downlink of asynchronous OFDM/FBMC based multi-cellular networks," *IEEE Trans. Wireless Commun.*, vol. 10, no. 8, pp. 2630–2639, Aug. 2011.

[7] P. Amini, R.-R. Chen, and B. Farhang-Boroujeny, "Filterbank multicarrier communications for underwater acoustic channels," *IEEE J. Ocean. Eng.*, vol. 40, no. 1, pp. 115–130, Jan. 2015.

[8] P. Siohan, C. Siclet, and N. Lacaille, "Analysis and design of OFDM/OQAM systems based on filterbank theory," *IEEE Trans. Signal Process.*, vol. 50, no. 5, pp. 1170–1183, May 2002.

[9] J. Du and S. Signell, "Novel preamble-based channel estimation for OFDM/OQAM systems," in *Proc. IEEE Int. Conf. Commun.*, Jun. 2009, pp. 1–6.

[10] D. Katselis, E. Kofidis, A. Rontogiannis, and S. Theodoridis, "Preamble-based channel estimation for CP-OFDM and OFDM/OQAM systems: A comparative study," *IEEE Trans. Signal Process.*, vol. 58, no. 5, pp. 2911–2916, May 2010.

[11] C. Lélé, J.-P. Javaudin, R. Legouable, A. Skrzypczak, and P. Siohan, "Channel estimation methods for preamble-based OFDM/OQAM modulations," *Eur. Trans. Telecommun.*, vol. 19, no. 7, pp. 741–750, 2008.

[12] E. Kofidis, D. Katselis, A. Rontogiannis, and S. Theodoridis, "Preamble-based channel estimation in OFDM/OQAM systems: A review," *Signal Process.*, vol. 93, no. 7, pp. 2038–2054, 2013.

[13] H. Lin, C. Lélé, and P. Siohan, "A pseudo alamouti transceiver design for OFDM/OQAM modulation with cyclic prefix," in *Proc. IEEE 10th Workshop Signal Process. Adv. Wireless Commun.*, Perugia, Italy, Jun. 2009, pp. 300–304.

[14] S. Alamouti, "A simple transmit diversity technique for wireless communications," *IEEE J. Sel. Areas Commun.*, vol. 16, no. 8, pp. 1451–1458, Oct. 1998.

[15] K. F. Lee and D. B. Williams, "A space-time coded transmitter diversity technique for frequency selective fading channels," in *Proc. IEEE Sensor Array Multichannel Signal Process. Workshop (SAM)*, Cambridge, MA, USA, Aug. 2000, pp. 149–152.

[16] N. Al-Dhahir, "Single-carrier frequency-domain equalization for space-time block-coded transmissions over frequency-selective fading channels," *IEEE Commun. Lett.*, vol. 5, no. 7, pp. 304–306, Jul. 2001.

[17] R. Zakaria and D. Le Ruyet, "On maximum likelihood MIMO detection in QAM-FBMC systems," in *Proc. IEEE PIMRC*, Instanbul, Turkey, Sep. 2010, pp. 183–187.

[18] R. Zakaria and D. Le Ruyet, "Intrinsic interference reduction in a filter bank-based multicarrier using QAM modulation," *Phys. Commun.*, vol. 11, pp. 15–24, Jun. 2014.

[19] H. Nam, M. Choi, S. Han, C. Kim, S. Choi, and D. Hong, "A new filter-bank multicarrier system with two prototype filters for QAM symbols transmission and reception," *IEEE Trans. Wireless Commun.*, vol. 15, no. 9, pp. 5998–6009, Sep. 2016.

[20] K. Zheng, L. Hou, H. Meng, Q. Zheng, N. Lu, and L. Lei, "Soft-defined heterogeneous vehicular network: Architecture and challenges," *IEEE Netw.*, vol. 30, no. 4, pp. 72–80, Jul. 2016.

[21] D. Sim, K. Kim, and C. Lee, "A layered detection algorithm based on interference cancellation for FBMC-QAM," *IEEE Commun. Lett.*, vol. 20, no. 10, pp. 1939–1942, Oct. 2016.
[22] R. Zakaria and D. Le Ruyet, "A novel filter-bank multicarrier scheme to mitigate the intrinsic interference: Application to MIMO systems," *IEEE Trans. Wireless Commun.*, vol. 11, no. 3, pp. 1112–1123, Mar. 2012.
[23] C. Lélé, P. Siohan, and R. Legouable, "The alamouti scheme with CDMA-OFDM/OQAM," *EURASIP J. Adv. Signal Process.*, vol. 2010, no. 1, p. 13, 2010.
[24] H. Nam, M. Choi, C. Kim, D. Hong, and S. Choi, "A new filter-bank multicarrier system for QAM signal transmission and reception," in *Proc. IEEE Int. Conf. Commun. (ICC)*, Sydney, NSW, Australia, Jun. 2014, pp. 5227–5232.
[25] I. Gaspar, M. Matthé, N. Michailow, L. L. Mendes, D. Zhang, and G. Fettweis, "Frequency-shift Offset-QAM for GFDM," *IEEE Commun. Lett.*, vol. 19, no. 8, pp. 1454–1457, Aug. 2015.
[26] X. Yang and B. Vucetic, "A frequency domain multi-user detector for TD-CDMA systems," *IEEE Trans. Commun.*, vol. 59, no. 9, pp. 2424–2433, Sep. 2011.
[27] K. Zheng, F. Liu, L. Lei, C. Lin, and Y. Jiang, "Stochastic performance analysis of a wireless finite-state Markov channel," *IEEE Trans. Wireless Commun.*, vol. 12, no. 2, pp. 782–793, Feb. 2013.
[28] F. Liu, K. Zheng, W. Xiang, and H. Zhao, "Design and performance analysis of an energy-efficient uplink carrier aggregation scheme," *IEEE J. Sel. Areas Commun.*, vol. 32, no. 2, pp. 197–207, Feb. 2014.
[29] K. Zheng, H. Meng, P. Chatzimisios, L. Lei, and X. Shen, "An SMDP-based resource allocation in vehicular cloud computing systems," *IEEE Trans. Ind. Electron.*, vol. 62, no. 12, pp. 7920–7928, Dec. 2015.

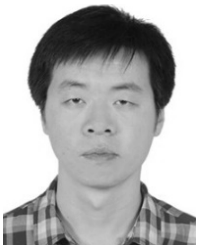

FEI LI received the M.S. degree in electronics engineering from Inner Mongolia University, China, in 2014. He is currently pursuing the Ph.D. degree with the Intelligent Computing and Communication Lab, Key Lab of Universal Wireless Communications, Ministry of Education, Beijing University of Posts and Telecommunications. His research interests lie on 5G wireless communication, such as new waveform and channel estimation.

KAN ZHENG (SM'09) received the B.S., M.S., and Ph.D. degree from the Beijing University of Posts and Telecommunications (BUPT), China, in 1996, 2000, and 2005, respectively. He is currently a Full Professor with BUPT. He has rich experiences on the research and standardization of new emerging technologies. He has authored over 200 journal articles and conference papers in the field of wireless networks, Internet-of-Things, and so on. He holds editorial board positions for several journals. He has also served in the Organizing/TPC Committees for more than 10 conferences, such as IEEE PIMRC, IEEE SmartGrid, and so on. He is currently the Chair of the IEEE Computer Society STC Internet-of-Everything.

HUI ZHAO received the M.S. degree from Tianjin University in 2003 and the Ph.D. degree from the Beijing University of Posts and Telecommunications (BUPT), China, in 2006. She is currently an Associate Professor with BUPT. She has accumulated rich experience in the field of LTE-advanced, ultra-high throughput WLAN, and 5G. Up to now, she has published over 80 papers in the journals and conferences and has owned 18 authorized patents.

WEI XIANG (SM'10) is currently a Foundation Professor and the Head of the Electronic Systems and Internet of Things Engineering Discipline. He is a fellow of IET and Engineers Australia.